ACS Macro Letters

Letter

pubs.acs.org/macroletters

Modeling Stretching-Induced Immiscibility in Nonmonodisperse Polymer Systems

Qun-li Lei,[†,§] Jia-wei Feng,[†,§] Hong-ming Ding,[†,‡] Chun-lai Ren,[*,†] and Yu-qiang Ma[*,†,‡]

[†]National Laboratory of Solid State Microstructures and Department of Physics, Collaborative Innovation Center of Advanced Microstructures, Nanjing University, Nanjing 210093, China

[‡]Center for Soft Condensed Matter Physics and Interdisciplinary Research, Soochow University, Suzhou 215006, China

Supporting Information

ABSTRACT: The behavior of polymer chains under stretching is a classical problem in polymer science. However, a fundamental question still in mist is how the stretching affects the interactions between polymer chains, especially when the tensions on the chains are unequal. In this work, we combine statistical theory and molecular simulations to study the influence of this tension disparity on the miscibility of athermal polymer systems. Through a minimal model, we demonstrate that when polymer chains of different lengths are under the same stretching disparate tension states among polymer chains can lead to either *macroscopic* or *microscopic* phase separation, depending on whether their ending points are mobile or not. Generally, the immiscibility found here is an entropic effect arising from conformational asymmetry between unequally stretched polymer chains. Our findings provide a new mechanism to explain the flow-induced demixing in polymer blends and indicate that heterogeneous structure can occur during stretching, simply as a result of nonmonodispersity in elastic polymer materials.

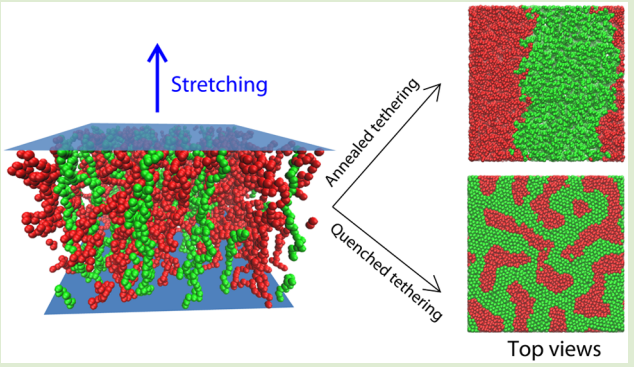

The phenomenon of polymer under stretching or tension not only is a persistent topic for elastic polymer materials, like rubber and plastics membrane, but also widely exists in polymer fluid,[1−3] polymer brush,[4−6] and polymer-mediated surface adhesion[7−9] etc. It was found that stretching can induce crystallization[10,11] or local orientational order[12,13] in rubber, which makes it an important fabricating process to increase the mechanical performance of polymer materials in modern industry.[14] Classical polymer theories[10,15] considering the decrease of entropy and orientational coupling during the stretching provided simple explanations for these stretching-induced phenomena. However, these venerable theories were based on the assumption that polymer chains are equally stretched. In reality, the tensions felt by individual polymer chains are far from uniform as a result of dispersion of polymer lengths and randomness of polymer network.[11,16,17] It is still unclear how this tension disparity modifies the thermodynamic property and microscopic structure of polymer materials.

Actually, the heterogeneous tension state is also a common feature in polymer rheology since free chains in polymer fluids are usually stretched by shear or extensional flows, which can be both spatially and temporally varied. Experimentally, complex flow-induced mixing and demixing phase behaviors[1,2] and even crystallization[3] were observed. Current explanations for these phenomena mainly relied on phenomenologically modified Flory−Huggins theories[18,19] or nonequilibrium methods.[20,21] Whether heterogeneous tension distribution in polymer fluid may contribute to the immiscibility has received little attention.

Therefore, a full comprehension of how the disparate tension states modify the miscibility of polymer systems is not only a fundamental question for polymer physics but also of great significance for the polymer industry. To answer this question, in this work, we build a minimal model wherein the tensions imposed on different polymer chains can be well tuned and studied. With the help from both theory and simulations, we show that disparate tension states are able to cause strong immiscibility and phase separation. The phase separation can be either microscopic or macroscopic, depending on whether the ends of polymer chains are mobile or not.

To model disparate tension states on different polymer chains, we tether two polymeric species, merely differing in length, on two opposite surfaces in an implicit solvent background, as illustrated in Figure 1. The tethering sites are mobile or fixed depending on the problem we study. Since we are only concerned about the entropic effect, the system is assumed to be athermal, and monomers simply interact with each other through excluded volume repulsion. Therefore, both the conformation and tension state of a polymer chain are

Received: July 10, 2015
Accepted: August 26, 2015
Published: September 1, 2015

DOI: 10.1021/acsmacrolett.5b00469
ACS Macro Lett. 2015, 4, 1033−1038

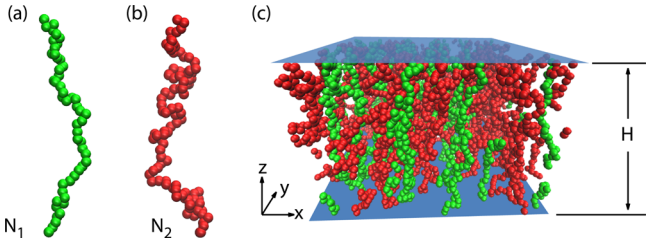

Figure 1. Schematic of the polymer-stretching system. (a) Short polymer molecules are represented by green chains with N_1 monomers. (b) Long polymer molecules are shown as red chains with N_2 monomers. (c) All polymer chains are attached to two opposite interfaces by their ending points.

mainly determined by two factors, i.e., the stretching distance, H, and the polymer length. Under the same H, short chains are expected to undertake higher tensions compared with long chains. By varying the length ratio between two polymer species as well as H, this model allows us to sensitively tune the tension disparity in the system.

We first assume that the tethering sites of polymer chains on the surfaces are mobile. To obtain the free energy of the system, we extend the statistical theory first raised by Di Marzio.[15] Under mean field approximation, the free energy of our ternary system can be written as

$$\frac{\beta v_0 F}{V} = -\frac{v_0(S_{c,1}+S_{c,2})}{k_B V} + \phi_s \ln \phi_s + \frac{\phi_1}{N_1}\ln\phi_1 + \frac{\phi_2}{N_2}\ln\phi_2 - \sum_{j=x,y,z}(1-\gamma_{1,j}\phi_1-\gamma_{2,j}\phi_2)\ln(1-\gamma_{1,j}\phi_1-\gamma_{2,j}\phi_2) \quad (1)$$

where $S_{c,1}$ and $S_{c,2}$ represent the configurational entropies of short and long polymer chains, respectively. The rest of the parts are the "packing entropy" according to the original Di Marzio theory. ϕ_s, ϕ_1, and ϕ_2 are the volume fractions of solvent background and two polymeric species. N_i is the monomer number of i species (i = 1,2), and v_0 is the volume of a monomer. Importantly, $\gamma_{i,j} = \alpha_{i,j}\frac{N_i-1}{N_i}$ reflects the anisotropic deformation of polymer chains of i species, with deformation parameter $\alpha_{i,j}$ defined as the fraction of monomers whose bond vectors point to the $\pm j$ direction ($j = x, y, z$). The stretching is assumed in the $+z$ direction and normal to the surface, which leads to $\alpha_{i,x} = \alpha_{i,y}$ by virtue of the symmetry of the system. On the basis of the three-chain model,[22] the deformation parameter $\alpha_{i,j}$ as a function of stretching distance H can be obtained as

$$\alpha_{i,x} = \alpha_{i,y} = \frac{1-\alpha_{i,z}}{2} \quad (2)$$

$$\alpha_{i,z} = \frac{2}{3}\sqrt{1+3\left(\frac{H}{L_i}\right)^2} - \frac{1}{3} \quad (3)$$

where $L_i = N_i b$ is the contour length of polymeric species i. As one can observe, if the stretching distance H is small, i.e., $H \ll L_i$, an isotropic distribution of segments' orientations is obtained, namely, $\alpha_{i,x} = \alpha_{i,y} = \alpha_{i,z} = \frac{1}{3}$. On the contrary, under a highly stretched situation $H \simeq L_i$, one would get $\alpha_{i,x} = \alpha_{i,y} = 0$ and $\alpha_{i,z} = 1$, indicating that chains are fully orientated toward the z direction. Details of the whole theory can be found in part 1 of the Supporting Information (SI).

Despite the mathematical simplicity, the theory presented here predicts that immiscibility can occur in the system due to disparate tension states among polymer chains. For the sake of clarification, we consider the simple binary polymer system ($\phi_1+\phi_2 = 1$) and assume $\frac{N_i-1}{N_i} \simeq 1$. Moreover, since the tension on more deformed chains f_1 is always larger than f_2 on less deformed chains (see part 2 of SI for the proof), intuitively, the deformation parameter $\alpha_{i,j}$ is rewritten as a function of the tension on polymer chain i, namely, $\alpha_{i,j} = \alpha_j(f_i)$. Through the second derivative of the free energy, one can find a shift to the location of the spinodal, which is generally viewed as the change of the effective Flory–Huggins χ_{12} parameter

$$\Delta\chi_{12} = \frac{[\alpha_z(f_1)-\alpha_z(f_2)]^2}{1-[\phi_1\alpha_z(f_1)+\phi_2\alpha_z(f_2)]^2} \quad (4)$$

In the long chain limit $L_2 > L_1 \gg H \gg b$, $\Delta\chi_{12}$ can be simplified to

$$\Delta\chi_{12} \simeq \frac{8b^4}{729(k_B T)^4}(f_1^2 - f_2^2)^2 \quad (5)$$

As can be observed, $\Delta\chi_{12}$ is always positive as long as the tensions on two polymer species are unequal, i.e., $f_1 \neq f_2$. This indicates that tension disparity decreases the miscibility of the system. If the disparity is large enough, strong immiscibility can induce a first-order phase separation.

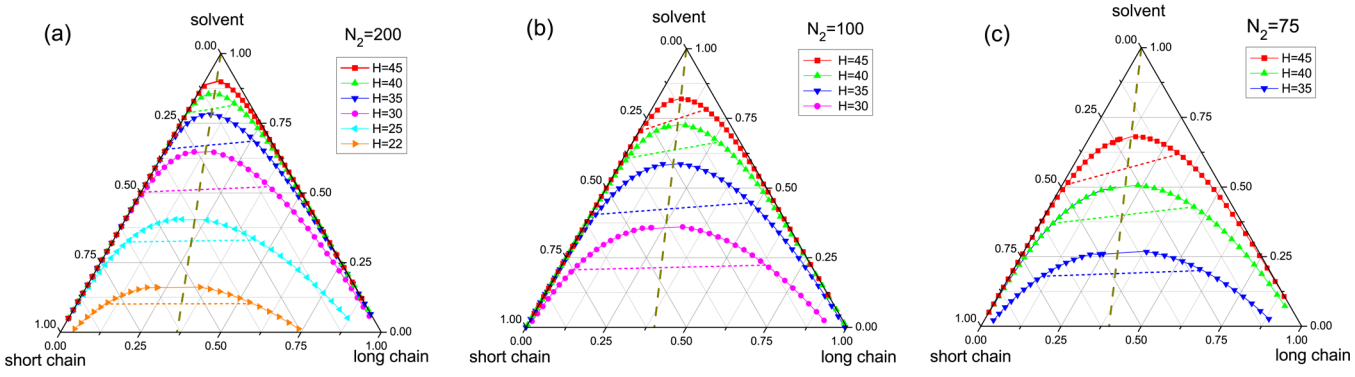

Figure 2. Theoretical phase diagrams for systems of different N_2 under varied stretching distances H with fixed $N_1 = 50$. The volume fraction of each component is the distance to its opposite side of the triangle. Every dotted line connects the two coexisting states. The dashed lines show the choices of initiative simulation states under different packing fractions.

DOI: 10.1021/acsmacrolett.5b00469
ACS Macro Lett. 2015, 4, 1033−1038

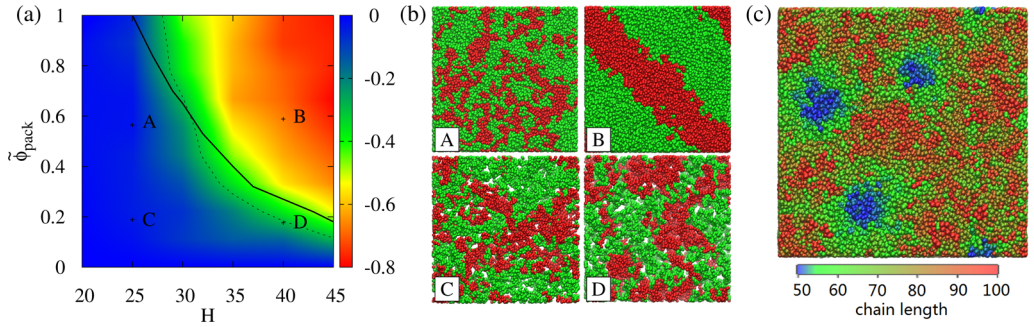

Figure 3. (a) Mixing parameter Γ (shown as color scales) as a function of $\tilde{\phi}_{pack}$ and H for $N_1 = 50$ and $N_2 = 100$. The dotted line represents Γ = −0.3, while the solid line shows theoretical calculations. Note that the real simulated packing fraction $\phi_{pack} = \rho\sigma^3$, which ranges from 0 to 0.85,[23] is normalized by $\tilde{\phi}_{pack} = \phi_{pack}/0.85$. (b) Top views of simulation systems for **A**, **B**, **C**, and **D** points in (a). (c) Top view of polymer melts system ($\tilde{\phi}_{pack} = 1$) of continual chain-length distribution under $H = 49$. Chains of different lengths are shown by different colors.

In order to explore this effect more deeply, we also design Brownian dynamics simulations of the system. Polymers are modeled as linear chains composed of coarse-grained beads. Neighboring beads are connected by harmonic bond potential $F_{bonded,i,i+1} = k_{bonded,i,i+1}(r_{i,j} - r_{i,j,0})^2$, with $k_{bonded}/kT = 128$ and $r_{i,j,0}/\sigma = 1$. A shifted Lennard-Jones potential, cut off at $2^{1/6}\sigma$, is used to model the repulsion between unconnected beads, i.e.

$$E_{nonbonded,i,j} = 4\epsilon\left[\left(\frac{\sigma}{r_{i,j}}\right)^{12} - \left(\frac{\sigma}{r_{i,j}}\right)^{6} + \frac{1}{4}\right] \qquad (r < 2^{1/6}\sigma)$$

where ϵ is chosen as $\epsilon/kT = 1$ and $\sigma = 1$. All beads are constrained inside the region $1 \le Z \le H + 1$ except for the ending beads of chains, which are restricted in $Z = 1$ and $Z = H + 1$ planes separatively. The dimensions of our simulation box are chosen as $50 \times 50 \times (H + 2)$ with periodic boundary conditions in three directions. The packing fraction $\phi_{pack} = \rho\sigma^3$ of polymer chains inside the box varies from 0 to 0.85,[23] where ρ is the total monomer density. All simulations are performed in the NVT ensemble by using the LAMMPS package (1 Feb 2014).[24] The time step is 0.01τ, and the data are collected every 100τ, with the total simulation time lager than $100\,000\tau$.

We first plot phase diagrams of general ternary systems in Figure 2 for chain lengths $N_1 = 50$ and $N_2 = 200$, 100, and 75, under various stretching distances H. For these three length ratios ($\kappa = N_2/N_1$), we find that as long as H reaches a critical value, a first-order phase transition occurs at high packing fraction ($\phi_{pack} = \phi_1 + \phi_2$), resulting in two coexisting phases with one rich in short chains and the other rich in long ones. Further increase of H enhances this immiscibility, making the coexisting curves shift to low packing fraction areas (the upper angle). On the other hand, when the length ratio κ is decreased from 4.0 ($N_2 = 200$) to 1.5 ($N_2 = 75$) under a fixed H, the phase separation is found to be significantly suppressed, resulting in a smaller phase transition area or even disappearing of it. The explanation for these results is that, although κ itself can not change the miscibility of system,[25] decreasing κ diminishes the tension disparity between two polymer species, which in turn weakens the immiscibility according to our former analysis. It should be mentioned that, generally, the external force is not the only factor leading to the stretching of polymer chains. Contribution from lateral intermolecular repulsion is also significant, especially in high tethering density circumstances. This issue is discussed in detail in part 1 of the SI.

In order to obtain more evidence from molecular level and further explore the dynamic aspect, we perform molecular simulations under different stretching H and packing fractions as well. The initiative proportions of two polymeric species are indicated by the dashed lines in Figure 2. To quantify the degree of demixing at the equilibrium state, we adopt a two-dimension mixing parameter Γ[26] by using the coordinates of chains' center points. This order parameter is based on the statistic of nearest neighbor numbers, which makes it highly suitable to characterize the mixing degree of the size-limited simulation system. The normalized Γ ranges from 0 to −1, representing the fully random-mixing state to the completely phase-separated state. For our systems, we find that when time-averaged Γ is below −0.3 segregation of the two polymeric species can be observed unambiguously. Therefore, Γ* = −0.3 can be tentatively regarded as an indicator of phase separation. In Figure 3a, we give Γ as a function of normalized $\tilde{\phi}_{pack}$ and H for $N_1 = 50$ and $N_2 = 100$ with the area of Γ < −0.3 enclosed by a dotted line. Top views of simulation systems for marked **A**, **B**, **C**, and **D** points in the phase diagram are given in Figure 3b (for lateral views, see Figure S1 in Supporting Information). For comparison, we also plot the theoretical critical packing fraction as a function of stretching, which is represented by a solid line in Figure 3a. It can be observed that our theoretical calculations agree well with simulation results. The same agreement is found for $N_1 = 50$ and $N_2 = 75$ systems (see Figure S2a), whereas for the large length ratio case ($N_1 = 50$, $N_2 = 200$) a discrepancy between simulations and theoretical calculations occurs in the area of high packing fraction and low stretching (see Figure S2b). This discrepancy seems to have a dynamic origin since the kinetics of phase transition is found to be much slower for highly packed systems when the stretching H approaches the critical value (Figure S3). Similar slow dynamics is found in other high-density systems near the critical point.[27] Nevertheless, the unperturbed chain assumption made in Di Marzio theory may also have a delicate influence on the phase behavior in high-density polymer systems, as discussed in part 1 of the SI.

With the help from molecular simulation, we also study a similar case wherein molecule number instead of packing fraction is fixed. In this situation, strong phase separation happens likewise (see movie S1 in Supporting Information). Furthermore, simulations enable us to explore the immiscibility in the system with continual tension distribution, where chains of different lengths ($N_i = 50, 51, ..., 99, 100$) are equally chosen. The snapshot is shown in Figure 3c. It can be observed that

DOI: 10.1021/acsmacrolett.5b00469
ACS Macro Lett. 2015, 4, 1033−1038

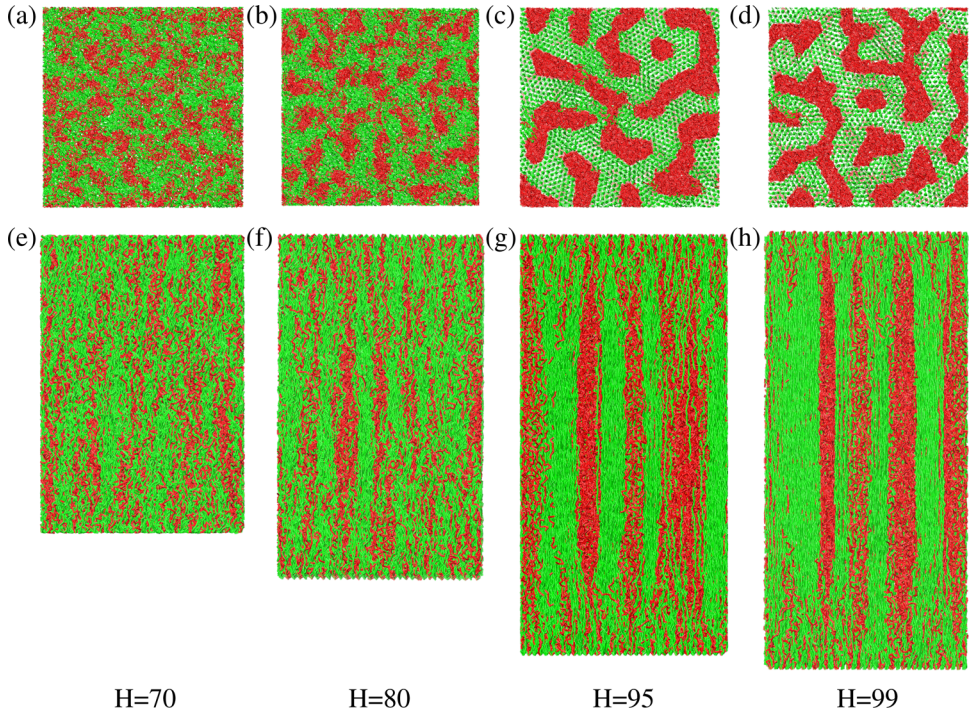

Figure 4. Top views of middle cross sections (up) and lateral views (down), for binary polymer mixtures with quenched tethering sites under different stretching distances: (a), (e) $H = 70$; (b), (f) $H = 80$; (c), (g) $H = 95$; (d), (h) $H = 99$. The tethering points are permanently fixed on 3 (short chain):1 (long chain) square lattices.

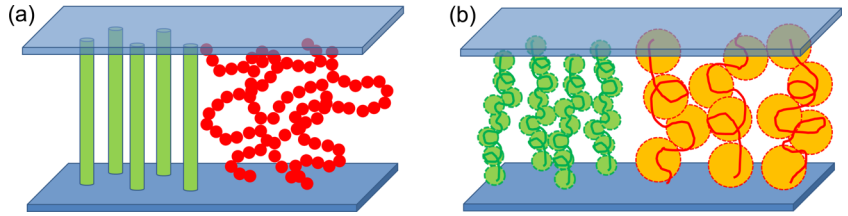

Figure 5. (a) Rigidity−disparity picture for short polymer chains under strong stretching. The immiscibility comes from favorable orientational coupling between more stretched chains. (b) Blob−disparity picture for long polymer chains under moderate stretching. The immiscibility between chains of dissimilar tension states can be understood as frustrated packing of tension blobs of unequal sizes.

short chains with high tension (blue) form compact aggregations, surrounded by chains of moderate tension (green) in the background of long and low-tension chains (red). Therefore, the stretching-induced immiscibility found in our bimodal tension distribution model is general and robust, which is the foundation to study real heterogeneous−tension state polymer systems.

The above theoretical and simulation studies are all based on the assumption that tethering sites of chains are mobile (annealed), which helps to quantify the stretching-induced immiscibility. Besides, this annealed system can be regarded as a minimal model for nonuniform stretching in polymer fluid. Copolymer systems with lamellar phase, where polymer chains are found to be strongly stretched,[28] may also provide the opportunity to directly test our predictions, if experiments are properly designed.

To further mimic the heterogeneous tension state in elastic polymer materials like rubber, we next study the case wherein the tethering points are immobile (quenched). The relaxation time of the quenched system is found to be faster than the annealed case since chains can only have local movements. This allows us to choose a relatively large simulation system with $N_1 = 100$ and $N_2 = 200$. In Figure 4, we give snapshots of binary polymer mixture systems at different stretching distances. The ratio of molecule numbers between short and long polymer chains is 3:1, which is the same as previous $N_1 = 50$ and $N_2 = 100$ systems, but the tethering sites of two polymeric species are permanently fixed in a square lattice (see Figure S4). Compared with annealed cases where *macroscopic* phase separation prevails, the quenched case shows *microscopic* phase separation when the stretching distance is increased from $H = 70$ to $H = 95$. The microscopic phase separation is a result of the competition between stretching-induced immiscibility and elastic constraints from quenched tethering points. Interestingly, even in a fully stretching situation ($H = 99$), clear microscopic phase morphology still exists. The reason is that the driving force for phase separation under $H = 99$ is so strong that short chains have to rearrange themselves at the cost of elastic energy of intramolecular bonds. Although the distribution of polymer length is still bimodal, it is expected that these phenomena also exist in polydisperse systems, similar to what happens in the annealed case of Figure 3c. Therefore, from a practical point, our results demonstrate that heterogeneous structure can occur during stretching, simply as a result of nonmonodispersity of polymer chains in elastic polymer materials. The microdomains in it could be nuclei of

DOI: 10.1021/acsmacrolett.5b00469
ACS Macro Lett. 2015, 4, 1033−1038

stretching-induced crystallization, as indicated by previous researches.[11,17]

So far, we have done a detailed investigation into the stretching-induced immiscibility in relatively short-chain systems with monomer number about 100. To observe phase separation, the stretching H should compare with N_1b for both annealed and quenched tethering cases. Under such conditions, stretched polymer chains of different tensions, in fact, can be regarded as chains of different rigidities; i.e., short chains under high tension behave like semirigid rods, while long chains with low tension still remain flexible (see Figure 5a). Immiscibility occurs as a result of local orientational coupling[29,30] between more stretched polymer chains, similar to what happens in rod−coil systems.[31,32]

Although this rigidity−disparity picture looks quite reasonable for short-chain systems, it may not be the case for long-chain ones. To explore this issue, we return to the binary polymer melts system. In the long-chain limit, $L_2 > L_1 \gg H \gg b$, different tethering ways (annealed or quenched) only play minor roles, and the critical stretching H^* can be obtained analytically based on eq 1 under the condition $\frac{\partial^2 F}{\partial^2 \phi_1} = \frac{\partial^3 F}{\partial^3 \phi_1} = 0$. The final expression is

$$H^* \simeq \sqrt{\frac{2(\sqrt{\kappa}+1)}{3(\kappa^2-1)}}\,\kappa^{3/4} N_1^{3/4} b \tag{6}$$

eq 6 gives a scaling relationship $H^* \sim N_1^{\nu}$ with $\nu = 3/4$. If we assume this scaling relationship is correct and turn to the blob picture, then the critical size of tension blobs ξ_1 is about $N_1^{1/4}b$ for short chains and $\xi_2 = \kappa\xi_1$ for long chains. The immiscibility in this long-chain system can not simply be attributed to the aforementioned orientational coupling since at the scale smaller than the size of the tension blob thermal fluctuations will make chains behave like random-walk without any orientational preferences.[25] Therefore, the immiscibility must come from the scale larger than the blob size. To understand this, one can image inserting a large blob into the space left open by removing some small blobs, or vice versa. The size difference between two kinds of blobs will cause an energetic frustration during the insertion.[33] This frustration gives rise to the immiscibility, similar to what happens in intrinsic conformational asymmetry systems.[33−35] Although the scaling factor $\nu = 3/4$ predicted by our mean-field theory requires further scrutiny, this blob−disparity picture holds as far as $\nu < 1$. Therefore, for long-chain systems under moderate stretching, the immiscibility is better to be interpreted as frustrated packing of tension blobs of unequal sizes (see Figure 5b).

Both the rigidity and blob disparities caused by tension inequality can be generally categorized as conformational asymmetry, which is a more general polymer physics issue[33−37] and exists in many other systems as well. For example, on cellular lipid membranes, lipid rafts are observed as a consequence of liquid−gel phase transition, which is driven by the conformational asymmetry between saturated and unsaturated lipids.[38] Intrinsic conformational asymmetry is also believed to be the main causation for phase behavior in mixtures of PE and PEE[33,35] and other molecules that are chemically similar but with different rigidities or topologies.[36,37] In fact, there is a strong formula similarity between expression of tension−disparity induced $\Delta\chi_{12} \propto (f_1^2 - f_2^2)^2$ in eq 5 and the theoretical result[33−35,37] $\Delta\chi_e \propto (\beta_1^2 - \beta_2^2)^2$ obtained from the intrinsic conformational asymmetry systems, where β_i is proportional to the chain's unperturbed gyration radius. This similarity is not an accident. On the contrary, it reveals a deeper physical connection between the conformational asymmetry and tension disparity. In part 3 of the SI, we give a tentative proof of this argument.

In conclusion, we present a minimal model to study how the disparate tension states arising from the difference of polymer lengths change the miscibility in the polymer-stretching system. Strong immiscibility and phase separation are predicted by statistical theory and confirmed by molecular simulations. The phase separation can be either macroscopic or microscopic by using different tethering methods. We demonstrate that this kind of immiscibility is an entropic effect resulting from the conformational asymmetry between unequally stretched polymer chains. For short-chain systems, the conformational asymmetry can be understood as that different tension states endow the chains with dissimilar rigidities, while for long-chain cases, frustrated packing of tension blobs of unequal sizes seems to be the right physical picture. Our findings provide a new point of view to understand the flow-induced demixing in polymer blends and indicate that heterogeneous structure can occur during stretching, simply as a result of nonmonodispersity in elastic polymer materials. Finally, a novel strategy to reversibly control the 3D microscopic morphology through external force is also demonstrated by our work, which may be useful for designing stretch-responded optical material,[39] directing the self-assembly of nanoparticles[40] and manipulating the conductivity of rechargeable lithium batteries.[41]

■ ASSOCIATED CONTENT

Supporting Information

The Supporting Information is available free of charge on the ACS Publications website at DOI: 10.1021/acsmacrolett.5b00469.

The details of our theory and supplementary data from molecular simulations (ZIP)

■ AUTHOR INFORMATION

Corresponding Authors

*E-mail: chunlair@nju.edu.cn.

*E-mail: myqiang@nju.edu.cn.

Author Contributions

§These authors contributed equally to this work.

Notes

The authors declare no competing financial interest.

■ ACKNOWLEDGMENTS

This work is supported by the National Natural Science Foundation of China (Nos. 91427302, 21274062, 91027040, 11474155) and the National Basic Research Program of China (No.2012CB821500). We are grateful to the High Performance Computing Center (HPCC) of Nanjing University for doing the numerical calculations in this paper on its IBM Blade cluster system.

■ REFERENCES

(1) Mani, S.; Malone, M. F.; Winter, H. H. *Macromolecules* **1992**, *25*, 5671−5676.

(2) Soontaranun, W.; Higgins, J. S.; Papathanasiou, T. D. *Fluid Phase Equilib.* **1996**, *121*, 273−292.

(3) Okura, M.; Mykhaylyk, O. O.; Ryan, A. J. *Phys. Rev. Lett.* **2013**, *110*, 087801.

DOI: 10.1021/acsmacrolett.5b00469
ACS Macro Lett. 2015, 4, 1033−1038

(4) Rabin, Y.; Alexander, S. *Europhys. Lett.* **1990**, *13*, 49−54.
(5) Singh, C.; Ghorai, P. K.; Horsch, M. A.; Jackson, A. M.; Larson, R. G.; Stellacci, F.; Glotzer, S. C. *Phys. Rev. Lett.* **2007**, *99*, 226106.
(6) Coluzza, I.; Hansen, J. P. *Phys. Rev. Lett.* **2008**, *100*, 016104.
(7) Kendall, K. *Molecular Adhesion and Its Applications*; Kluwer Academic Publishers: Norwell, MA, 2004.
(8) Jeppesen, C.; Wong, J. Y.; Kuhl, T. L.; Israelachvili, J. N.; Mullah, N.; Zalipsky, S.; Marques, C. M. *Science* **2001**, *293*, 465−468.
(9) Ding, H. M.; Ma, Y. Q. *Biomaterials* **2012**, *33*, 5798−5802.
(10) Flory, P. J. *J. Chem. Phys.* **1947**, *15*, 397−408.
(11) Candau, N.; Laghmach, R.; Chazeau, L.; Chenal, J. M.; Gauthier, C.; Biben, T.; Munch, E. *Macromolecules* **2014**, *47*, 5815−5824.
(12) Jarry, J. P.; Monnerie, L. *Macromolecules* **1979**, *12*, 316−320.
(13) Deloche, B.; Samulski, E. T. *Macromolecules* **1981**, *14*, 575−581.
(14) Baer, E.; Hiltner, A.; Keith, H. D. *Science* **1987**, *235*, 1015−1022.
(15) Dimarzio, E. A. *J. Chem. Phys.* **1962**, *36*, 1563.
(16) Tosaka, M. *Polym. J.* **2007**, *39*, 1207−1220.
(17) Zhang, M. M.; Zha, L. Y.; Gao, H. H.; Nie, Y. J.; Hu, W. B. *Chin. J. Polym. Sci.* **2014**, *32*, 1218−1223.
(18) Wolf, B. A. *Macromolecules* **1984**, *17*, 615−618.
(19) Rangelnafaile, C.; Metzner, A. B.; Wissbrun, K. F. *Macromolecules* **1984**, *17*, 1187−1195.
(20) Onuki, A. *Phys. Rev. Lett.* **1989**, *62*, 2472−2475.
(21) Helfand, E.; Fredrickson, G. H. *Phys. Rev. Lett.* **1989**, *62*, 2468−2471.
(22) James, H. M.; Guth, E. *J. Chem. Phys.* **1943**, *11*, 455−481.
(23) Baljon, A. R. C.; Grest, G. S.; Witten, T. A. *Macromolecules* **1995**, *28*, 1835−1840.
(24) Plimpton, S. *J. Comput. Phys.* **1995**, *117*, 1−19.
(25) Rubinstein, M.; Colby, R. *Polymer Physics*; Oxford University Press: USA, 2003.
(26) Liu, Z. Y.; Guo, R. H.; Xu, G. X.; Huang, Z. H.; Yan, L. T. *Nano Lett.* **2014**, *14*, 6910−6916.
(27) Coppock, P. S.; Kindt, J. T. *J. Phys. Chem. B* **2010**, *114*, 11468−11473.
(28) Goveas, J. L.; Milner, S. T.; Russel, W. B. *Macromolecules* **1997**, *30*, 5541−5552.
(29) Sotta, P.; Deloche, B.; Herz, J.; Lapp, A.; Durand, D.; Rabadeux, J. C. *Macromolecules* **1987**, *20*, 2769−2774.
(30) Olmsted, P. D.; Milner, S. T. *Macromolecules* **1994**, *27*, 6648−6660.
(31) Flory, P. J. *Macromolecules* **1978**, *11*, 1138−1141.
(32) Lei, Q. L.; Ren, C. L.; Su, X. H.; Ma, Y. Q. *Sci. Rep.* **2015**, *5*, 9217.
(33) Bates, F. S.; Fredrickson, G. H. *Macromolecules* **1994**, *27*, 1065−1067.
(34) Fredrickson, G. H.; Liu, A. J.; Bates, F. S. *Macromolecules* **1994**, *27*, 2503−2511.
(35) Singh, C.; Schweizer, K. S. *J. Chem. Phys.* **1995**, *103*, 5814.
(36) Dudowicz, J.; Freed, K. F.; Douglas, J. F. *Phys. Rev. Lett.* **2002**, *88*, 095503.
(37) Wang, Z. G. *J. Chem. Phys.* **2002**, *117*, 481−500.
(38) Alberts, B.; Johnson, A.; Lewis, J.; Raff, M.; Roberts, K.; Walte, P. In *Molecular Biology of the Cell*; Anderson, M., Granum, S., Eds.; Garland science: New York, 2008.
(39) Pursiainen, O. L. J.; Baumberg, J. J.; Winkler, H.; Viel, B.; Spahn, P.; Ruhl, T. *Adv. Mater.* **2008**, *20*, 1484.
(40) Grzelczak, M.; Vermant, J.; Furst, E. M.; Liz-Marzan, L. M. *ACS Nano* **2010**, *4*, 3591−3605.
(41) Inceoglu, S.; Rojas, A. A.; Devaux, D.; Chen, X. C.; Stone, G. M.; Balsara, N. P. *ACS Macro Lett.* **2014**, *3*, 510−514.

DOI: 10.1021/acsmacrolett.5b00469
ACS Macro Lett. 2015, 4, 1033−1038